



Cite this: *Polym. Chem.*, 2022, **13**, 2554

## Organic–inorganic hybrid nanomaterials prepared via polymerization-induced self-assembly: recent developments and future opportunities

Bing Niu, <sup>a</sup> Ying Chen, <sup>b</sup> Li Zhang <sup>a,b</sup> and Jianbo Tan <sup>a,b</sup>

Organic–inorganic hybrid nanomaterials are an important class of functional materials that find applications in many areas. Cooperative self-assembly of inorganic nanoparticles and block copolymers in solution is one of the most widely employed approaches for preparing organic–inorganic hybrid nanomaterials with precise structures and properties. However, this method usually encounters problems with low solids contents (<1% w/w) and multi-step processes, and is difficult to implement on a large scale. Over the past decade or so, the development of polymerization-induced self-assembly (PISA) has enabled the preparation of concentrated block copolymer nanomaterials (10–50% w/w solids) with a diverse set of morphologies. This review focuses on recent developments in the preparation of organic–inorganic hybrid nanomaterials via PISA including: (i) post-modification of block copolymer nanoparticles, (ii) *in situ* encapsulation of inorganic nanoparticles into vesicles, (iii) cooperative self-assembly of inorganic nanoparticles and polymers. By highlighting these important developments, the current challenges and future opportunities of organic–inorganic hybrid nanomaterials prepared via PISA are also provided.

Received 11th February 2022,  
Accepted 1st April 2022

DOI: 10.1039/d2py00180b

[rsc.li/polymers](http://rsc.li/polymers)

## 1. Introduction

Nanoscience has made significant progress over the past twenty years, and researchers have been able to control the preparation of nanomaterials with various structures such as nanospheres, nano-mesoporous materials, nanowires, hollow nanotubes, core–shell structural nanomaterials and so on.<sup>1–10</sup> Since the size of nanomaterials is close to the wavelength of light and the coherence length of electrons, materials at the nanoscale exhibit different properties compared to bulk materials.<sup>11</sup> Hybrid nanomaterials are emerging multifunctional nanomaterials that usually integrate with two or more dissimilar materials,<sup>12,13</sup> and typically they are inorganic components and organic components. Inorganic components usually include gold, silica, iron oxide, quantum dots, *etc.*,<sup>14</sup> while organic components usually include ligands, biomolecules, polymers, *etc.*<sup>15,16</sup>

The development of self-assembly techniques provides more opportunities for diverse applications of nanomaterials. Self-assembly usually refers to basic units (*i.e.*, nanomaterials and block copolymers) that spontaneously form an ordered

structure through the interaction of non-covalent bonds (*i.e.*, hydrogen bonding, hydrophobic interactions, and  $\pi$ – $\pi$  interactions).<sup>17–21</sup> In particular, the cooperative self-assembly of polymers and inorganic nanoparticles in solution has proved to be one of the most efficient methods to prepare organic–inorganic hybrid nanomaterials with unique structures and properties.<sup>22–30</sup> However, the cooperative self-assembly method is usually conducted in a highly dilute solution (<1% w/w) with multi-step processes, which is not beneficial for the large-scale preparation and application of organic–inorganic hybrid nanomaterials.

Over the past decade or so, the development of polymerization-induced self-assembly (PISA) has enabled the preparation of concentrated block copolymer nanomaterials (10–50% w/w solids) with a diverse set of morphologies including spheres, worms, vesicles, large-compound vesicles, nanotubes, *etc.*<sup>31–82</sup> During PISA, the formation and *in situ* self-assembly of block copolymers occur at the same time, making the mechanism of PISA much more complicated than the traditional self-assembly method. A variety of polymerization techniques has been introduced into PISA including reversible addition–fragmentation chain transfer (RAFT) polymerization,<sup>31,35,83</sup> atom transfer radical polymerization (ATRP),<sup>84,85</sup> nitroxide mediated polymerization (NMP),<sup>86,87</sup> ring-opening metathesis polymerization (ROMP),<sup>88,89</sup> ring-opening polymerization (ROP),<sup>90,91</sup> living anionic polymerization (LAP),<sup>92</sup> and organotellurium-mediated radical polymer-

<sup>a</sup>Department of Polymeric Materials and Engineering, School of Materials and Energy, Guangdong University of Technology, Guangzhou 510006, China.  
E-mail: tanjianbo@gdut.edu.cn

<sup>b</sup>Guangdong Provincial Key Laboratory of Functional Soft Condensed Matter, Guangzhou 510006, China

ization (TERP).<sup>93</sup> Numerous PISA reviews on various topics have been published over the past several years.<sup>94–115</sup> Over the past ten years, PISA has been employed to prepare organic–inorganic hybrid nanomaterials at high solids contents, and it can overcome the problems of the traditional cooperative self-assembly method. In this review, we summarize the recent developments in the preparation of organic–inorganic hybrid nanomaterials based on PISA including the post-modification method *via* either *in situ* reduction or absorption, *in situ* encapsulation of inorganic nanoparticles into vesicles, and cooperative self-assembly of inorganic nanoparticles and polymers. Finally, the current challenges and future opportunities are also provided.

## 2. Post-modification method

In PISA, functional groups could be introduced to the surface and inner regions of block copolymer nano-objects using functional macro-CTAs and functional monomers, respectively.<sup>107</sup> The presence of these functional groups can be used to anchor inorganic nanoparticles *via* either *in situ* reduction or absorption, allowing the large-scale preparation of organic–inorganic hybrid nanomaterials with a diverse set of morphologies. Table 1 summarizes organic–inorganic hybrid nanomaterials prepared by the post-modification method.

The An group<sup>116</sup> prepared  $\beta$ -ketoester functional nanospheres and vesicles by thermally initiated RAFT dispersion polymerization of 2-(acetoacetoxy)ethyl methacrylate (AEMA) at high monomer concentrations (20–30%). Taking advantage of the unique structure of the  $\beta$ -ketoester group that can be used to achieve metal complexation, silver nanoparticles could be formed within the block copolymer nano-objects *via* *in situ*

reduction (Fig. 1). Recently, block copolymer nano-objects with embedded  $\beta$ -ketoester groups have also been prepared by the photoinitiated RAFT dispersion polymerization of AEMA and isobornyl methacrylate (IBOMA) at low temperatures.<sup>117</sup> The  $\beta$ -ketoester-functionalized block copolymer nano-objects were then cross-linked with a certain amount of ethylenediamine and the unreacted  $\beta$ -ketoester groups were further used to coordinate lanthanide ions in a good solvent (tetrahydrofuran in this case). Lanthanide-doped block copolymer vesicles with luminescence and magnetic properties were successfully prepared.

Semsarilar *et al.*<sup>118</sup> reported the efficient synthesis of block copolymer vesicles using a poly(methacrylic acid) (PMAA) macromolecular chain transfer agent (macro-CTA). After mixing alumina-coated silica nanoparticles (Ludox CL) with the anionic vesicles, the vesicles armored with different payloads of silica nanoparticles could be obtained. Karagöz *et al.*<sup>119</sup> synthesized poly(oligoethylene glycol methacrylate)-*b*-poly(methacrylic acid)-*b*-polystyrene (POEGMA-*b*-PMAA-*b*-PSt) triblock copolymer nano-objects with worm-like and vesicular morphologies. Carboxyl groups on the surface of block copolymer nano-objects were used to complex an iron ion mixture. Iron oxide nanoparticles/nanocomposites exhibiting high transverse relativities were prepared by alkaline coprecipitation of  $\text{Fe}^{\text{II}}$  and  $\text{Fe}^{\text{III}}$  salts (Fig. 2). Yu *et al.*<sup>120</sup> prepared mono-disperse poly(methyl methacrylate) (PMMA) microspheres by photoinitiated RAFT dispersion polymerization using poly(acrylic acid) (PAA) as the macro-CTA. Europium-doped lanthanum fluoride nanoparticles ( $\text{LaF}_3:\text{Eu}$ ) with photoluminescence properties have been employed to prepare various functional materials.<sup>137</sup>  $\text{LaF}_3:\text{Eu}$ /PMMA nanocomposites were then prepared by depositing  $\text{LaF}_3:\text{Eu}$  nanoparticles onto PMMA microspheres. It was found that increasing the number of carboxyl

**Table 1** Summary of organic–inorganic hybrid nanomaterials prepared *via* the post-modification method

Entry	Block copolymer	Functional group	Inorganic component	Morphology	Ref.
1	POEGMA-PAEMA	$\beta$ -Ketoester group	Ag	S, V	116
2	PHPMA-P(AEMA- <i>co</i> -IBOMA)	$\beta$ -Ketoester group	Tb, Ho	V	117
3	PMAA-PBzMA	Carboxyl group	$\text{SiO}_2$	V	118
4	POEGMA- <i>b</i> -PMAA- <i>b</i> -PSt	Carboxyl group	$\text{Fe}_2\text{O}_3$	W, V	119
5	PAA-PMMA	Carboxyl group	$\text{LaF}_3:\text{Eu}$	S	120
6	PAA-PSt	Carboxyl group	Ag	V	121
7	POEGMA-PDMAEMA-PSt	Tertiary amine group	Au	S, W, V	122
8	PDMAEMA-PSt	Tertiary amine group	$\text{SiO}_2$	W	123
9	PDMAEMA-PSt	Tertiary amine group	Au, $\text{SiO}_2$ , $\text{TiO}_2$	S	124
10	PDMAEMA-PBzMA	Tertiary amine group	$\text{SiO}_2$	S	125
11	PGMA-P(HPMA- <i>co</i> -DMAEMA)	Tertiary amine group	$\text{SiO}_2$	V	126
12	PHPMA-PDEMA	Tertiary amine group	Au	S, W, V	127
13	mPEG- <i>b</i> -PDMAEMA- <i>b</i> -PHPMA	Tertiary amine group	Au, Pd	S	128
14	$\beta$ -CD-POEGMA-PHPMA (PCMS- <i>g</i> -P4VP)- <i>b</i> -PSt	$\beta$ -CD	Au	S, W, V	129
15	mPEG-P(St- <i>co</i> -4VP)	Pyridine group	Au	S	130
16	EDA/mPEG-PGMA	Pyridine group	Ag	V	131
17	Succinic acid/POEOMA- <i>b</i> -P(PHFEMA- <i>co</i> -GMA)	Amine group	Ag	V	132
18	PMPS-PBzMA	Carboxyl group	$\text{Fe}_3\text{O}_4$	S	133
19	mPEG-PtBA	Alkoxysilane	$\text{SiO}_2$	S, W, V	134
20	Segmented PDMA-PSt	Trithiocarbonate group	Ag	V	135
21		Trithiocarbonate group	Ag	V	136

S: Spheres, W: Worms, and V: Vesicles.

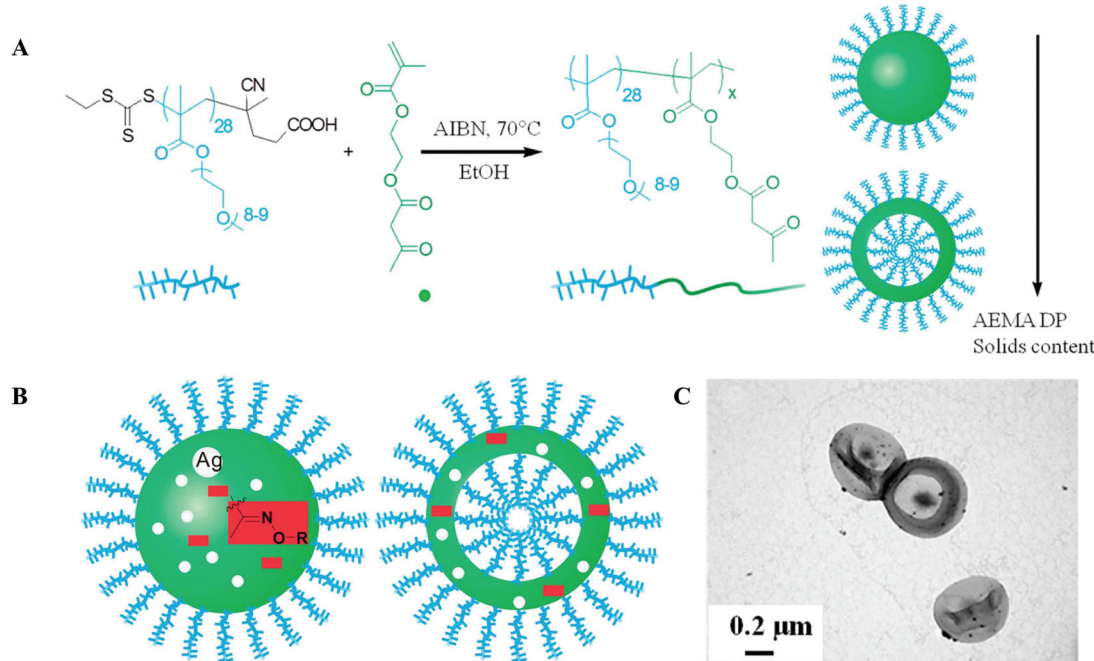


**Fig. 1** (A and B) Organic–inorganic hybrid materials were prepared by *in situ* formation of Ag nanoparticles within POEGMA-PAEMA vesicles. (C) TEM image of the prepared Ag-loaded vesicles. Reproduced with permission from ref. 116. Copyright © 2014, American Chemical Society.

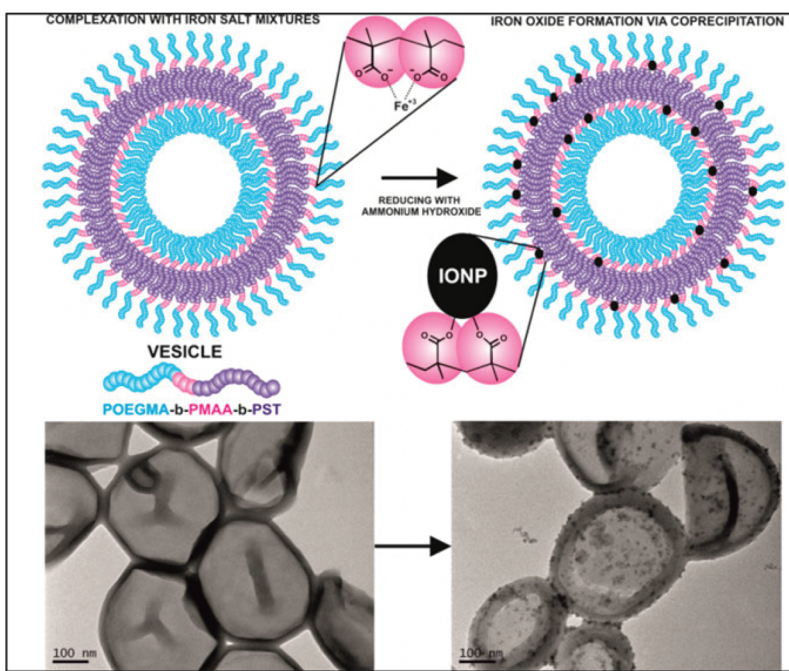


**Fig. 2** Schematic illustration of the iron complexation and iron oxide formation in POEGMA-*b*-PMAA-*b*-PSt triblock copolymer vesicles. Reproduced with permission from ref. 119. Copyright © 2014, American Chemical Society.

groups on the surface promoted the formation of hollow  $\text{LaF}_3$ :Eu/PMMA nanocomposites. After dissolving  $\text{LaF}_3$ :Eu nanoparticles in  $\text{HNO}_3$ , the hollow  $\text{LaF}_3$ :Eu/PMMA nanocomposites transformed into solid microspheres with smooth surfaces again. Tan *et al.*<sup>121</sup> reported a one-pot synthesis of PAA-PSt or

PAA-P(St-*co*-AA) block copolymer nano-objects with various morphologies. Taking advantage of the interaction between Ag nanoparticles and the carboxyl group as well as the unique properties (*i.e.* catalytic and antibacterial properties) of Ag nanoparticles,<sup>138,139</sup> the carboxyl-functional block copolymer

nano-objects were further used as substrates to prepare Ag/polymer nanocomposites. The obtained Ag/polymer nanocomposites can be used to reduce 4-nitrophenol in the presence of NaBH<sub>4</sub>.

Au nanoparticles have broad applications in catalysis, biological imaging, and energy storage due to their good biocompatibility and high photothermal conversion efficiency.<sup>140–142</sup> Bleach *et al.*<sup>122</sup> synthesized poly(oligoethylene glycol methacrylate)-*b*-poly(2-(dimethylamino)ethyl methacrylate)-*b*-polystyrene (POEGMA-PDMAEMA-PSt) triblock copolymer nano-objects by RAFT dispersion polymerization with tertiary amine groups located on the corona. Au/polymer nanocomposites were prepared by the *in situ* reduction of HAuCl<sub>4</sub> using NaBH<sub>4</sub>. The composition of Au nanoparticles in these Au/polymer nanocomposites could be further tuned by changing the concentration of chloroauric acid. Silica nanotubes have important applications in adsorption, catalysis, medicine and other fields due to their large specific surface areas, high aspect ratios and hollow structures. However, the large-scale preparation of silica nanotubes is challenging.<sup>143–146</sup> Zhang *et al.*<sup>123</sup> synthesized a series of PDMAEMA-PSt diblock copolymer nanowires by RAFT dispersion polymerization using a PDMAEMA macro-CTA. Then, the PDMAEMA corona on the surface of nanowires was used to catalyze the condensation polymerization of tetraethyl orthosilicate (TEOS), allowing the preparation of silica/polymer hybrid nanowires. After the calcination of these hybrid nanowires at 500 °C, silica nanotubes could be obtained (Fig. 3). Zhang *et al.*<sup>124</sup> also employed PISA-made PDMAEMA-PSt block copolymer nanoparticles as templates to prepare various inorganic–organic hybrid nanoparticles. Recently, our group<sup>126</sup> prepared CO<sub>2</sub>-responsive cross-linked vesicles by aqueous photoinitiated RAFT dispersion polymerization of 2-hydroxypropyl methacrylate (HPMA) and DMAEMA. Taking advantage of the interaction

between silica nanoparticles and tertiary amine groups, hybrid vesicles were obtained by mixing silica nanoparticles with the vesicles. The payload of silica nanoparticles could be significantly increased after protonating the tertiary amine group *via* CO<sub>2</sub> treatment.

Huang *et al.*<sup>127</sup> reported the synthesis of photocrosslinkable and amine-containing block copolymer nano-objects by the RAFT dispersion polymerization of 2-((3-(4-(diethylamino)phenyl)acryloyloxy)ethyl methacrylate (DEMA). The block copolymer nano-objects could be crosslinked *via* UV irradiation and further employed as templates for the *in situ* preparation of Au/polymer hybrid nanomaterials. Wan *et al.*<sup>128</sup> synthesized mPEG-PDMAEMA-PHPMA triblock copolymer nano-objects with tertiary amine groups on the surface by ultrasound-initiated RAFT dispersion polymerization (Fig. 4). The obtained amine-functionalized block copolymer nano-objects were further employed as scaffolds for *in situ* reduction of metal ions (including Au and Pd ions) by radicals *via* sonolysis of H<sub>2</sub>O. The Au/polymer and Pd/polymer hybrid nanomaterials formed showed excellent catalytic properties on aerobic alcohol oxidation and the Suzuki–Miyaura cross-coupling reaction, respectively.

Shi *et al.*<sup>130</sup> synthesized multicompartiment nanoparticles of the brush block terpolymer of [poly(*p*-chloromethylstyrene)-graft-poly(4-vinylpyridine)]-*b*-polystyrene (PCMS-*g*-P4VP)-*b*-PSt *via* RAFT dispersion polymerization of St (Fig. 5). Au nanoparticles were immobilized on the PCMS-*g*-P4VP domains to form Au/polymer hybrid nanomaterials. The obtained Au/polymer hybrid nanomaterials exhibited high catalytic efficiency in the oxidation of aerobic alcohols. Huang *et al.*<sup>131</sup> prepared large compound vesicles by the RAFT dispersion polymerization of St and 4VP mediated by a binary mixture of a macro-CTA and a CTA. Ag nanoparticles were attached to the large compound vesicles *via* the *in situ* reduction of AgNO<sub>3</sub>.

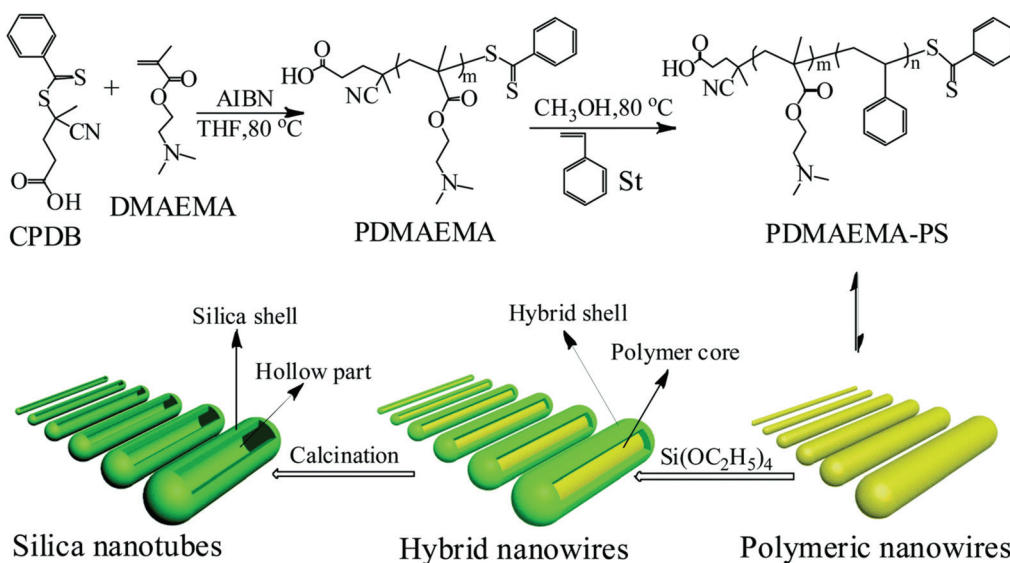


**Fig. 3** Schematic illustration of the synthesis of PDMAEMA-PSt block copolymer nanowires and their application in the preparation of silica/PDMAEMA-PSt hybrid nanowires and silica nanotubes. Reproduced with permission from ref. 123. Copyright © 2014, Royal Society of Chemistry.

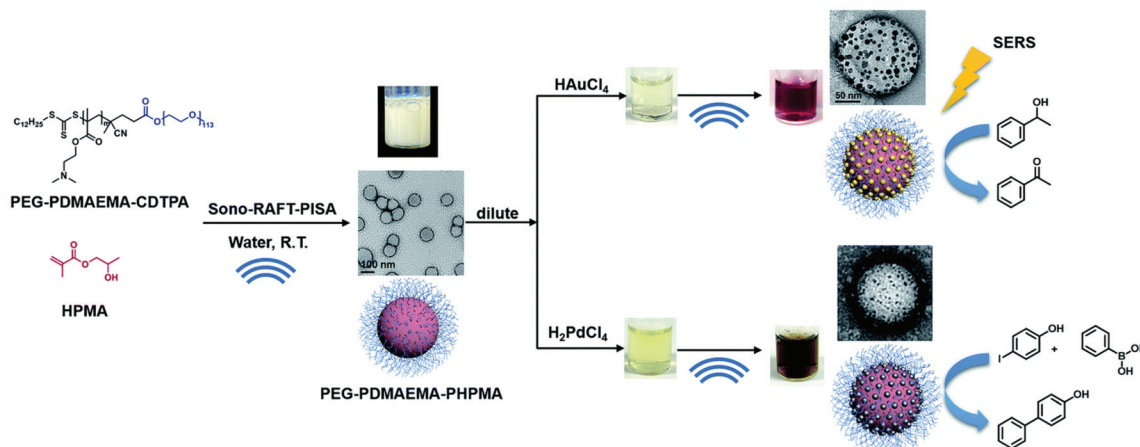


**Fig. 4** Schematic illustration of the synthesis of mPEG-PDMAEMA-PHPMA triblock copolymer nano-objects by sono-RAFT PISA, and the preparation of Au and Pd nanocomposites by ultrasound. Reproduced with permission from ref. 128. Copyright © 2021, Royal Society of Chemistry.

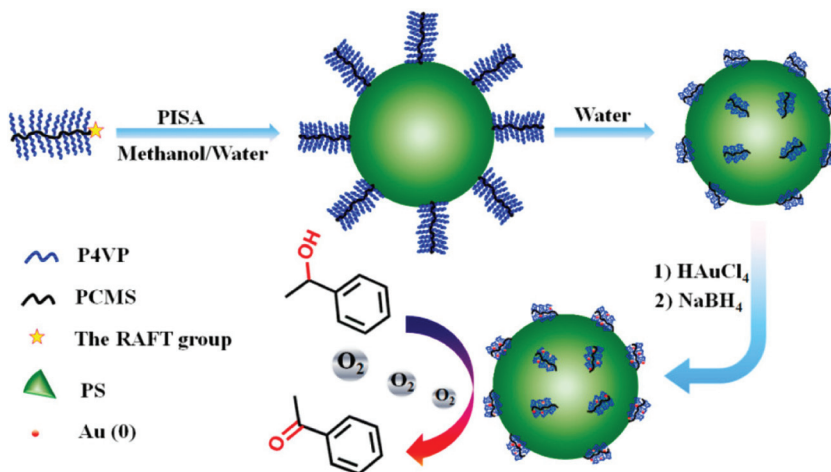


**Fig. 5** Schematic illustration of the synthesis of (PCMS-g-P4VP)-b-PSt nanoparticles by PISA and the preparation of Au nanocomposites. Reproduced with permission from ref. 130. Copyright © 2015, American Chemical Society.

using  $\text{NaBH}_4$ . The obtained Ag/polymer hybrid nanomaterials also exhibited excellent catalytic properties by reducing methylene blue with  $\text{NaBH}_4$ .

Tan *et al.*<sup>132</sup> reported the first PISA formulation of glycidyl methacrylate (GlyMA) to prepare epoxy-functionalized block copolymer nano-objects with various morphologies at room temperature. Cross-linked and amine-functionalized block copolymer nano-objects could be obtained by treatment with excess ethylene diamine (EDA) *via* the epoxy-amine chemistry. The obtained amine-functionalized block copolymer nano-objects were further used as templates to prepare Ag/polymer hybrid nanomaterials *via* *in situ* reduction of  $\text{AgNO}_3$  that exhibited good catalytic properties. Shi *et al.*<sup>133</sup> developed initiators for continuous activator regeneration (ICAR) ATRP-based dispersion polymerization of 2-(perfluorohexyl)ethyl methacrylate (PFHEMA) and GlyMA for the synthesis of epoxy-functionalized block copolymer nano-objects (Fig. 6). After the

introduction of carboxyl groups into the core-forming block *via* epoxy-thiol chemistry,  $\text{Fe}^{2+}$  and  $\text{Fe}^{3+}$  ions were loaded into the incorporated carboxyl groups, and  $\text{NH}_3 \cdot \text{H}_2\text{O}$  was added to form  $\text{Fe}_3\text{O}_4$  nanoparticles within the block copolymer nano-objects.

It is well known that RAFT groups (e.g., trithiocarbonate group) have strong interactions with metal ions, which can be used to anchor heavy metal nanoparticles onto block copolymer nano-objects prepared by RAFT-mediated PISA.<sup>147,148</sup> However, RAFT groups usually embed inside block copolymer nano-objects in most RAFT-mediated PISA formulations due to the use of R-type macro-RAFT agents (the solvophilic block is connected to the fragmenting group of the RAFT agent), which makes it difficult to prepare organic–inorganic hybrid nanomaterials based on the RAFT groups. To overcome this problem, one attractive strategy is the utilization of a Z-type macro-RAFT agent (the solvophilic block is connected to the

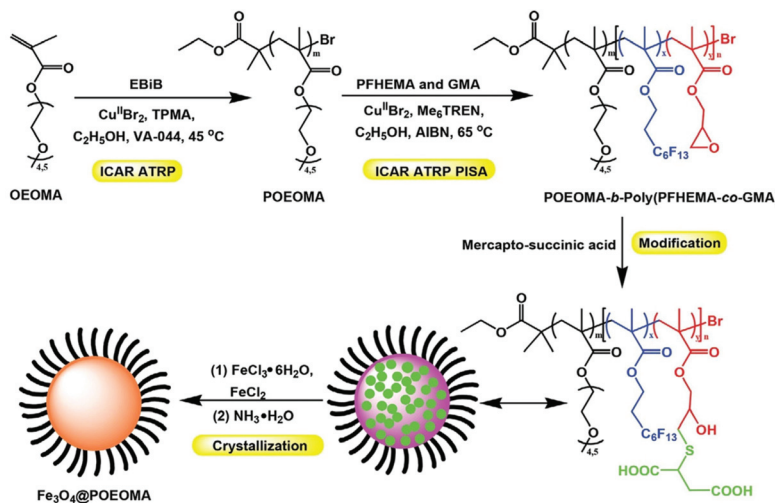


**Fig. 6** Preparation scheme of  $\text{Fe}_3\text{O}_4$  nanoparticles within the block copolymer nano-objects. Reproduced with permission from ref. 133. Copyright © 2019 WILEY-VCH Verlag GmbH & Co. KGaA, Weinheim.

non-fragmenting group of the RAFT agent) in RAFT-mediated PISA. Our group<sup>135</sup> developed the first well-controlled Z-RAFT-mediated dispersion polymerization using a Z-type macro-RAFT agent. In this formulation, all RAFT groups were located on the surface of block copolymer nano-objects. Ag/polymer hybrid nanomaterials were successfully prepared by attaching Ag nanoparticles on the block copolymer nano-objects *via* the *in situ* reduction of  $\text{AgNO}_3$  in the presence of poly(*N*-vinylpyrrolidone). Very recently, we synthesized segmented macro-RAFT agents using an asymmetric difunctional small molecular RAFT agent.<sup>136</sup> These segmented macro-RAFT agents were used to mediate the RAFT dispersion polymerization of St and various block copolymer nano-objects were obtained. Due to the unique structure of the segmented macro-RAFT agent, a certain number of RAFT groups could be introduced to the surfaces of block copolymer nano-objects. These block copolymer nano-objects were also used as scaffolds to prepare Ag/polymer hybrid nanomaterials *via* the *in situ* reduction of  $\text{AgNO}_3$  (Fig. 7). As a control experiment, block copolymer nano-objects prepared by RAFT dispersion polymerization using a traditional macro-RAFT agent were also employed to prepare Ag/polymer hybrid nanomaterials. However, no silver nanoparticles were observed on the block copolymer nano-objects due to the absence of RAFT groups on the surface.

### 3. *In situ* encapsulation of inorganic nanoparticles into vesicles

Block copolymer vesicles are hollow nanospheres with a bilayer structure that have broad applications in drug delivery, nanoreactors, Pickering emulsions, catalysis, sensing, and so on.<sup>149–151</sup> In the morphological phase diagram of PISA, the phase of vesicles usually occupies a very large region at high solids contents.<sup>152–154</sup> There is a natural fit for the efficient

preparation of vesicles by PISA at high solids contents. Moreover, the Armes group<sup>155</sup> reported that vesicles evolved from anisotropic worms during PISA and a “jellyfish” intermediate morphology is usually observed. Therefore, it is possible to prepare inorganic nanoparticle-loaded hybrid vesicles by encapsulating nanoparticles into vesicles *via* PISA.

Our group<sup>156,157</sup> reported the first *in situ* encapsulation of inorganic nanoparticles into vesicles by PISA. Silica nanoparticles were added at the beginning of aqueous photoinitiated RAFT dispersion polymerization of 2-hydropropyl methacrylate (HPMA) at room temperature using a monomethoxy poly(ethylene glycol) (mPEG) macro-CTA (Fig. 8). Transmission electron microscopy (TEM) characterization showed that the presence of silica nanoparticles had no influence on the formation of the vesicular morphology. Unloaded silica nanoparticles could be removed *via* several centrifugation–resuspension cycles. Taking advantage of the high electron contrast of silica nanoparticles, TEM analysis confirmed the successful formation of silica nanoparticle-loaded hybrid vesicles. Silica nanoparticle-loaded hybrid vesicles can also be prepared by enzyme-initiated aqueous RAFT dispersion polymerization at room temperature.<sup>158</sup> Almost at the same time, the Armes group<sup>159</sup> also reported the successful preparation of silica nanoparticle-loaded hybrid vesicles by the aqueous RAFT dispersion polymerization of HPMA using a poly(glycerol methacrylate) (PGMA) macro-CTA. TEM, cryo-TEM, small-angle X-ray scattering (SAXS), and disc centrifuge sedimentometry (DCP) were employed to characterize the silica nanoparticle-loaded vesicles formed. They demonstrated that the loading efficiency determined by TGA was consistent with that determined by either SAXS or DCP. Ding *et al.*<sup>160</sup> synthesized tubular Ag/polymer hybrid nanomaterials by the RAFT dispersion polymerization of St in poly(ethylene glycol) using a poly(*N*-isopropylacrylamide) macro-CTA. They found that adding Ag nanoparticles in RAFT dispersion

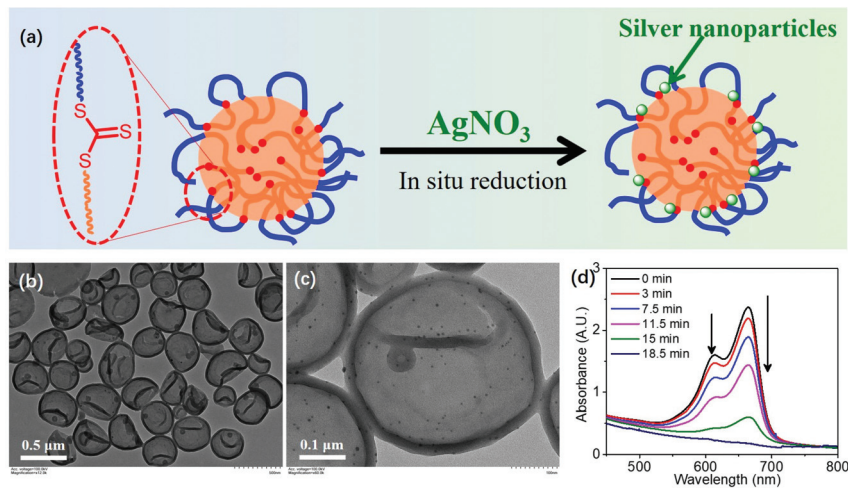


**Fig. 7** (a) Schematic illustration of the *in situ* reduction of  $\text{AgNO}_3$  on the surface of block copolymer nano-objects. (b and c) TEM images of Ag hybrid vesicles prepared *via* *in situ* reduction of  $\text{AgNO}_3$ . (d) UV-vis spectra of methylene blue reduced by  $\text{NaBH}_4$  using the Ag hybrid vesicles. Reproduced with permission from ref. 136. Copyright © 2022, American Chemical Society.

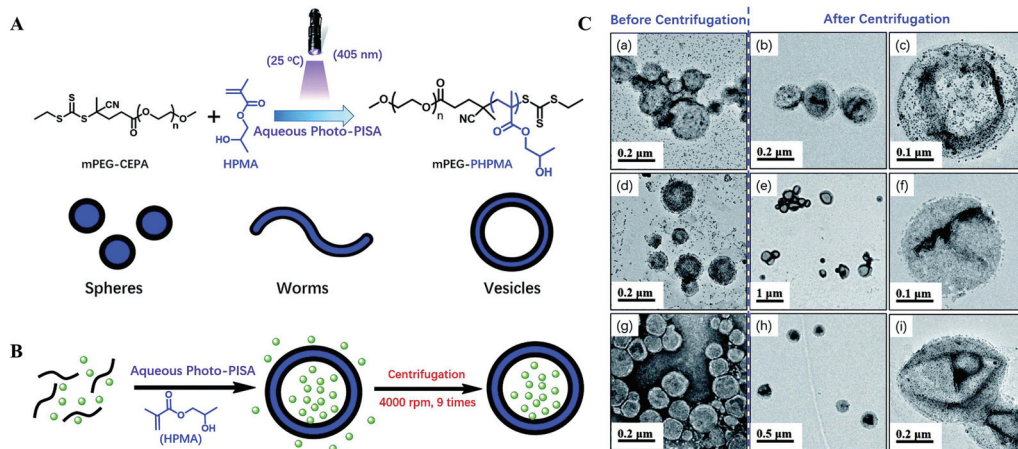


**Fig. 8** (A and B) Schematic illustration of the preparation of hybrid vesicles loaded with silica nanoparticles *via* aqueous photo-PISA of HPMA. (C) TEM images of unpurified and purified  $\text{mPEG}_{113}\text{-PHPMA}_{365}$  hybrid vesicles prepared *via* aqueous photo-PISA of HPMA by adding different amounts of silica sol. Reproduced with permission from ref. 157. Copyright © 2017, Royal Society of Chemistry.

polymerization had little effect on the polymerization kinetics. In contrast, the addition of Ag nanoparticles had a significant effect on the morphology of Ag/polymer hybrid nanomaterials (Fig. 9).

For some specific applications, it is necessary to release inorganic nanoparticles from vesicles under mild conditions. For example, the controlled release of silica nanoparticles from polymer vesicles has potential to repair living tissues or hydrogels *via* a self-repair mechanism.<sup>161</sup> To achieve this goal, we copolymerized a certain amount of DMAEMA with HPMA in aqueous photoinitiated RAFT dispersion polymerization to obtain silica nanoparticle-loaded hybrid vesicles.<sup>157</sup> After treatment with  $\text{CO}_2$  at room temperature for 2 min, the vesicular membrane disassembled into dissolved block copolymers due to the protonation of the tertiary amine, leading to the release

of silica nanoparticles from vesicles. Taking advantage of the thermo-responsive property of PHPMA, the Armes group<sup>159</sup> induced the morphology change from vesicles to worms or spheres after incubating the silica nanoparticle-loaded PGMA-PHPMA vesicles at low temperatures (0–10 °C), leading to the release of silica nanoparticles from vesicles. The same group<sup>162</sup> further investigated the kinetics of thermally triggered release of silica nanoparticles from vesicles using time resolved SAXS. They found that the payload of silica nanoparticles inside PGMA-PHPMA vesicles could lead to different thermally triggered morphological transitions. Deng *et al.*<sup>163</sup> used the dynamic covalent chemistry of phenylboronic acids with *cis*-diols to induce vesicle-to-worm/sphere transition, which could also release silica nanoparticles from PGMA-PHPMA vesicles (Fig. 10).

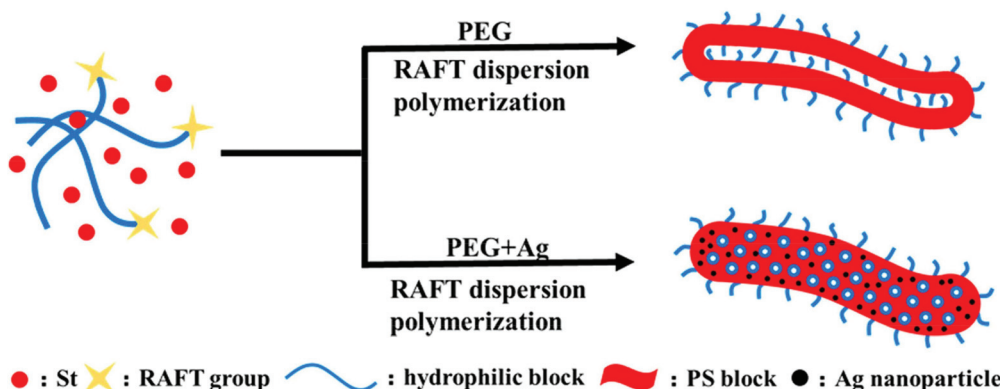


Fig. 9 Schematic illustration of the synthesis of coil–coil diblock copolymer nanotubes and tubular Ag/polymer nanocomposites. Reproduced with permission from ref. 160. Copyright © 2017, American Chemical Society.

In contrast to aqueous RAFT dispersion polymerization, RAFT emulsion polymerization should be a more versatile method that can help prepare block copolymer nano-objects in water using various hydrophobic monomers.<sup>96</sup> However, kinetically trapped spheres are usually obtained by RAFT emulsion polymerization. Recently, the Armes group<sup>164</sup> and our group<sup>165</sup> reported that the aqueous solubility of monomers played an important role in the morphological evolution from lower-order morphologies to higher-order morphologies during RAFT-mediated emulsion polymerization. Our group<sup>166</sup> successfully synthesized silica nanoparticle-loaded hybrid vesicles by adding silica nanoparticles at the beginning of the photoinitiated RAFT emulsion polymerization of *tert*-butyl acrylate (*t*BA) at room temperature. The Hawkett group<sup>167</sup> encapsulated a titanium dioxide ( $\text{TiO}_2$ ) pigment into vesicles by RAFT emulsion polymerization for the preparation of  $\text{TiO}_2$  nanoparticle-loaded vesicles. 100% loading efficiency was achieved in this formulation and the obtained  $\text{TiO}_2$  nanoparticle-loaded vesicles were employed as enhanced opacifiers in water-borne painting.

The above examples demonstrated that hybrid vesicles with inorganic nanoparticle loading inside could be conveniently

prepared by PISA. The stabilizer block located on the surface of hybrid vesicles enables the distribution of these nanoparticles in different media or substrates. Ning *et al.*<sup>168</sup> prepared silica nanoparticle-loaded poly(methacrylic acid)-poly(benzyl methacrylate) (PMAA-PBzMA) vesicles by PISA in ethanol or ethanol/water. The silica nanoparticle-loaded vesicles were further used to mediate the crystallization of  $\text{CaCO}_3$ , leading to the formation of  $\text{CaCO}_3$  single crystals with silica nanoparticles embedded inside (Fig. 11). It is noteworthy that the Armes group has recently reviewed the preparation of organic–inorganic hybrid materials by efficient occlusion of block copolymer nanoparticles within inorganic single crystals.<sup>115</sup>

#### 4. Cooperative self-assembly of inorganic nanoparticles and polymers

During PISA, the synthesis and *in situ* self-assembly of block copolymers occur at the same time. Therefore, the *in situ* self-assembly process can be precisely controlled by tuning the polymerization kinetics.<sup>75</sup> Moreover, the cooperative self-

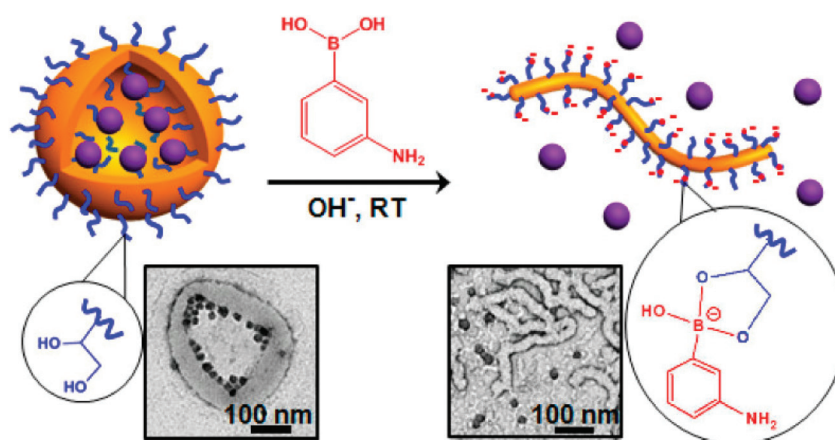
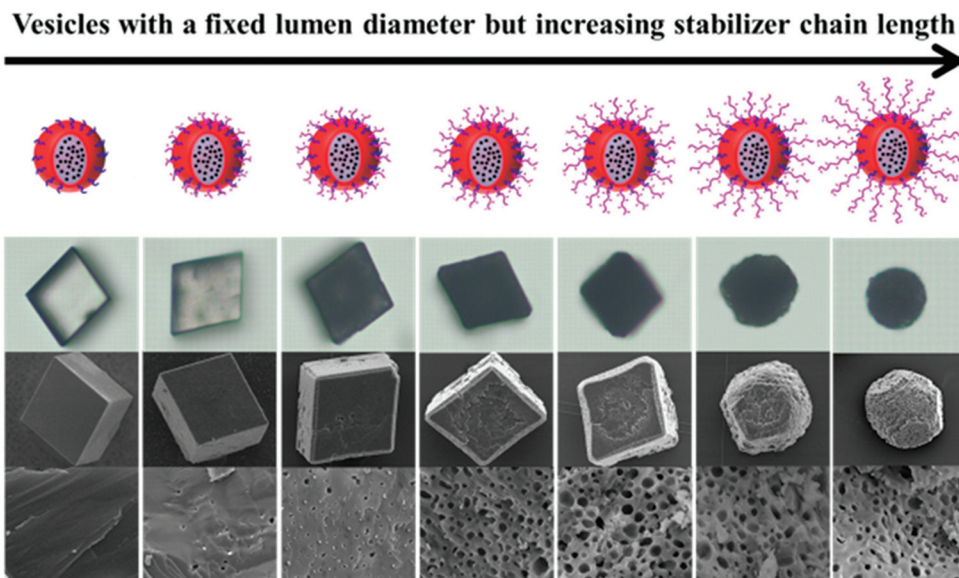


Fig. 10 Release of silica nanoparticles from PGMA-PHPMA vesicles via the dynamic covalent chemistry of phenylboronic acids with *cis*-diols. Reproduced with permission from ref. 163. Copyright © 2017, American Chemical Society.



**Fig. 11** Anionic block copolymer vesicles for efficient occlusion in calcite: the effects of different chain lengths of poly(methacrylic acid) on the  $\text{CaCO}_3$  crystal morphology. Reproduced with permission from ref. 168. Copyright © 2019, American Chemical Society.

assembly of different types of polymers can be achieved by mixing different macro-CTAs or CTAs, leading to the formation of different types of polymer nanomaterials.<sup>47,169–172</sup> The unique features of PISA provide a facile platform to prepare organic–inorganic hybrid nanomaterials using inorganic nanoparticles with macro-CTAs or CTAs on the surface.

Zheng *et al.*<sup>173</sup> grafted a poly(2-hydroxyethyl methacrylate) (PHEMA) brush on the surface of silica nanoparticles by RAFT polymerization. Subsequently, RAFT groups at the end of the PHEMA brush were removed, and additional RAFT agents were further modified on the surface of silica nanoparticles. The obtained silica nanoparticle-based macro-CTAs were dispersed in methanol to mediate the polymerization-induced self-assembly of benzyl methacrylate (BzMA). With the continuous increase of the molecular weight of PBzMA, each silica nanoparticle became more and more solvophobic, and cooperative self-assembly occurred to decrease the interfacial energy between the PBzMA chains and the solvent. Finally, worm-like organic–inorganic hybrid nanoparticles were formed (Fig. 12). To improve the stabilizing effect, the same group<sup>174</sup> conducted the PISA of BzMA in ethanol using PHPMA-grafted silica nanoparticles instead of PHEMA-grafted silica nanoparticles. In this case, the authors observed the formation of silica nanoparticle vesicles during the PISA process (Fig. 13). However, in these systems, the polymerization system became unstable as the monomer conversion increased, and the final monomer conversion was extremely low (<15%). Moreover, the silica nanoparticles were relatively polydisperse, which is not beneficial for the formation of well-defined organic–inorganic hybrid nanomaterials. Recently, Wang *et al.*<sup>175</sup> proposed a cooperative self-assembly strategy for preparing superstructures of inorganic–organic hybrid nanomaterials. Through DPD simulations, they found that ring, disk, and

composite superstructures could be obtained by changing the grafting density of the nanoparticles. Dynamics, thermodynamics, and structural details in the cooperative self-assembly process are also shown.

Recently, Hou *et al.*<sup>176</sup> reported a novel PISA system that was mediated by a mixture of linear macro-CTAs dissolved in the reaction medium and macro-CTAs grafted on the surface of silica nanoparticles (220 nm). As shown in Fig. 14, with the growth of the solvophobic block (PSt in this case), there are two competitive PISA processes that occurred in the system. To lower the interfacial energy, cooperative self-assembly of the block copolymer brush on the surface of silica nanoparticles and the free block copolymers in the reaction medium occurs, leading to the formation of organic–inorganic hybrid nanomaterials with block copolymer micelles attached on the surface of silica nanoparticles. Meanwhile, a certain number of stable block copolymer micelles was also formed during the PISA process, which can be removed *via* several centrifugation–redispersion cycles. The morphologies of organic–inorganic hybrid nanocomposites can be controlled by changing the molecular weights of the solvophilic block and the solvophobic block. Using a similar strategy, the same group<sup>177</sup> performed PISA mediated by a mixture of a linear macro-CTA dissolved in the reaction medium and CTA-grafted silica nanoparticles. In this case, asymmetric organic–organic hybrid nanoparticles with tunable anisotropy were formed.

Qiao *et al.*<sup>178,179</sup> reported the first nitroxide-mediated synthesis of silica/polymer nanocomposites by surfactant-free emulsion polymerization of St and *n*-butyl methacrylate. In this study, a brush-type macro-alkoxyamine initiator composed of poly(ethylene oxide) methacrylate (PEGMA) and a small amount of St was first synthesized and then adsorbed on the surface of silica nanoparticles through hydrogen-bonding

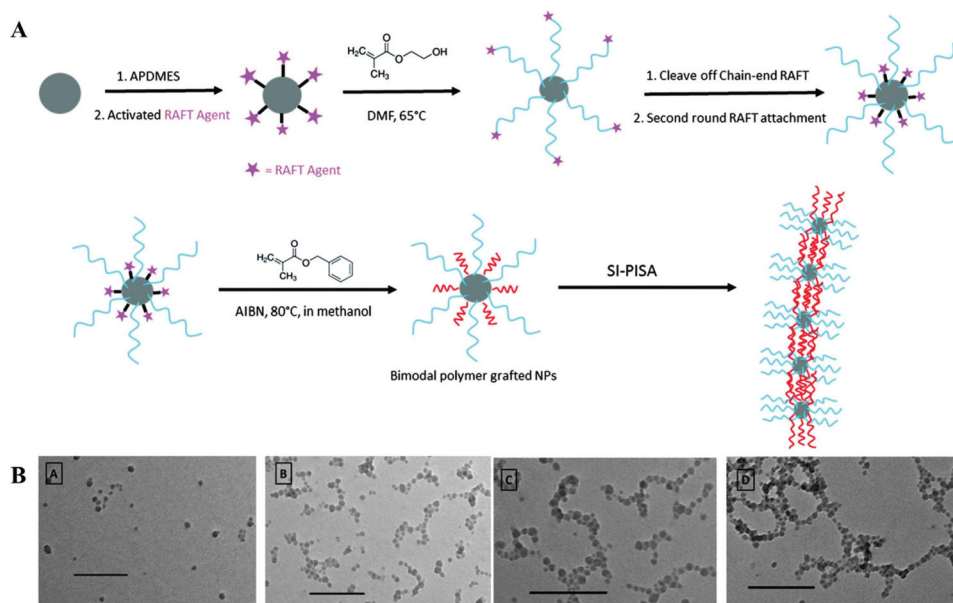


**Fig. 12** (A) Surface-initiated RAFT dispersion polymerization of BzMA and HEMA from  $\text{SiO}_2$  nanoparticles in methanol. (B) TEM images of the morphologies formed at 0 h, 1.5 h, 2 h, and 4.5 h. Reproduced with permission from ref. 173. Copyright © 2016, Royal Society of Chemistry.

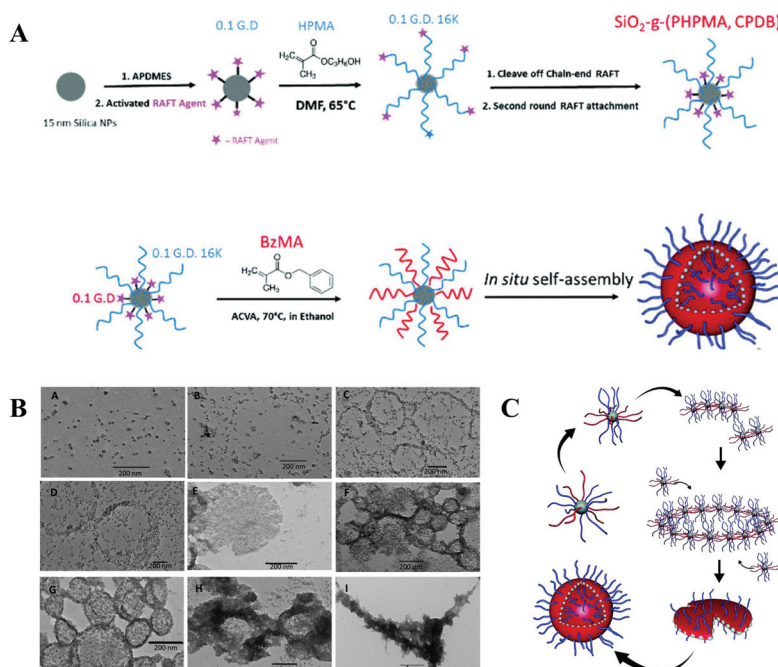


**Fig. 13** (A) Synthesis of inorganic nanoparticle vesicles via surface-initiated polymerization-induced self-assembly. (B) TEM images of the cooperative self-assembly at different polymerization times. (C) The mechanisms of cooperative self-assembly. Reproduced with permission from ref. 174. Copyright © 2017, Royal Society of Chemistry.

interactions. Using these adsorbed macro-alkoxyamine initiators in surfactant-free emulsion polymerization, silica nanoparticles with block copolymer micelles distributed on the surface were formed. The morphologies of the formed organic-inorganic hybrid nanomaterials could be further tuned by changing the macroinitiator concentration or the size

of silica nanoparticles. This strategy is also versatile for surfactant-free RAFT-mediated emulsion polymerization using PEG-based macro-RAFT agents.<sup>180</sup> It was found that changing the composition of the macro-RAFT agent led to different adsorptions to the silica nanoparticles. Therefore, the morphologies of silica/polymer nanocomposites could be tuned using

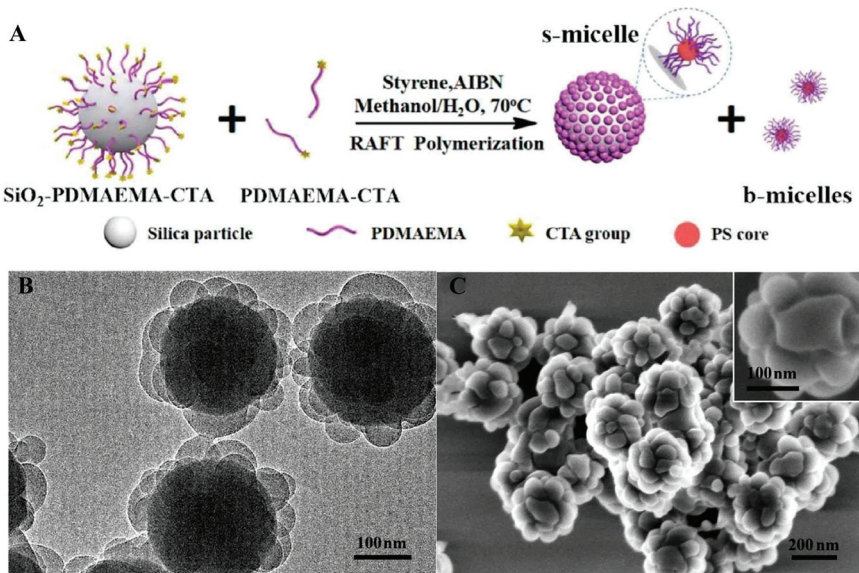


Fig. 14 (A) Schematic diagram of polymerization-induced surface self-assembly. (B) TEM and (C) high-resolution SEM images of hybrid silica particles. Reproduced with permission from ref. 176. Copyright © 2019, American Chemical Society.

different macro-RAFT agents. Upadhyaya *et al.*<sup>181</sup> reported the synthesis of PMAA-PMMA diblock copolymers *via* RAFT-mediated PISA in the presence of Fe<sub>2</sub>O<sub>3</sub> nanoparticles. They found that Fe<sub>2</sub>O<sub>3</sub> nanoparticles were decorated on the block copolymer nanoparticles. The formed hybrid nanoparticles were further used to prepare thin film membranes for water filtration.

Recently, Liu *et al.*<sup>182</sup> synthesized Janus Au@block copolymer nanoparticles by UV-initiated RAFT-mediated PISA (Fig. 15). Firstly, a P4VP-based macro-RAFT agent was synthesized and employed to functionalize the citrate-capped Au nanoparticles. The obtained Au nanoparticles were further used to mediate the RAFT dispersion polymerization of St under UV light irradiation. As the polymerization proceeded, the size of the polymer part of the Janus Au@block copolymer nanoparticles increased.

## 5. Current challenges and future opportunities

With the development of PISA over the past ten years or so, more and more simple and feasible strategies have been explored for the preparation of organic–inorganic hybrid nanomaterials with diverse morphologies and functionalities. As discussed in the previous sections, there are mainly three strategies for preparing organic–inorganic hybrid nanomaterials based on PISA including the post-modification strategy, *in situ* encapsulation of inorganic nanoparticles into vesicles, and cooperative self-assembly of inorganic nanoparticles and polymers. Although great progress has been made in the preparation of organic–inorganic hybrid nanomaterials *via* PISA,

there are still many challenges and possible opportunities in this research area.

The post-modification method using PISA-made block copolymer nano-objects as scaffolds is a facile and scalable method to prepare organic–inorganic hybrid nanomaterials. However, it is very difficult to precisely control the payload of inorganic nanoparticles, the size of inorganic nanoparticles, and the distribution of inorganic nanoparticles within hybrid nanomaterials. Moreover, inorganic nanoparticles cannot anchor strongly to the polymer scaffolds due to relatively weak interactions. To overcome these problems, the development of novel PISA systems that can form block copolymer nano-objects with precise sizes and functionalities by PISA is desirable. For example, Manners *et al.*<sup>183</sup> successfully developed polymerization-induced crystallization-driven self-assembly (PI-CDSA), allowing the efficient synthesis of uniform fiber-like micelles and block copolymer micelles. The PI-CDSA provides a potential method to control the distribution of inorganic nanoparticles within the hybrid nanomaterials. Moreover, introducing functional groups into block copolymer nano-objects that can strongly anchor to inorganic nanoparticles is also an attractive strategy to enhance the stability of organic–inorganic hybrid nanomaterials.

The *in situ* encapsulation of inorganic nanoparticles into vesicles *via* PISA is an attractive strategy to prepare organic–inorganic hybrid nanomaterials that may find applications in some specific areas. Until now, only SiO<sub>2</sub> and TiO<sub>2</sub> nanoparticles have been encapsulated into vesicles *via* PISA. Moreover, only limited approaches have been developed to release inorganic nanoparticles from vesicles. To expand the versatility of this strategy, the *in situ* encapsulation of other inorganic nanoparticles and the development of other stimulus-

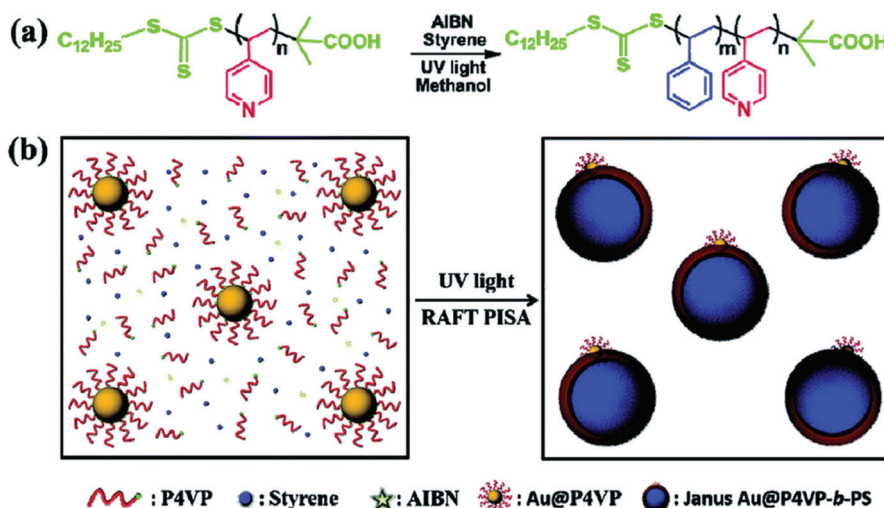


Fig. 15 Schematic illustration for (a) the synthesis of P4VP-b-PSt block copolymers and (b) the synthesis of Janus Au@block copolymer nanoparticles by UV-initiated PISA. Reproduced with permission from ref. 182. Copyright © 2021, Royal Society of Chemistry.

responsive vesicles that can release inorganic nanoparticles are encouraged.

The cooperative self-assembly of inorganic nanoparticles and polymers by PISA is a potential strategy that can precisely result in the preparation of organic-inorganic hybrid nanomaterials. Due to the intrinsic mechanism of PISA in which polymerization and self-assembly occur simultaneously, the mechanism of cooperative self-assembly of inorganic nanoparticles and polymers in PISA is complicated. One important current state-of-the-art is the detailed investigation of the mechanism of this unique process by various characterization techniques such as TEM, size exclusion chromatography (SEC), SAXS, dynamic light scattering (DLS), TGA, etc. The effects of the reaction parameters on the morphologies of the hybrid nanomaterials should also be studied in detail.

Finally, we note that organic-inorganic hybrid nanomaterials prepared based on PISA have shown potential applications in various areas such as catalysis, functional coating, biomaterialization, etc.<sup>132,167,168</sup> It would be fascinating to explore the applications of these organic-inorganic hybrid nanomaterials in other areas such as drug delivery, water purification, sensing, stimuli-responsive hydrogels and so on.

## Conflicts of interest

There are no conflicts to declare.

## Acknowledgements

The authors acknowledge support from the National Natural Science Foundation of China (Grant 22171055 and 21971047), the Guangdong Natural Science Foundation for Distinguished Young Scholar (Grant 2022B1515020078), the Science and Technology Program of Guangzhou (Grant 202102020631), and

the Innovation Project of Education Department in Guangdong (Grant 2018KTSCX053). Y. C. acknowledges the support from the Guangdong Special Support Program (2017TX04N371).

## References

- 1 A. J. Heinrich, W. D. Oliver, L. M. K. Vandersypen, A. Ardavan, R. Sessoli, D. Loss, A. B. Jayich, J. Fernandez-Rossier, A. Laucht and A. Morello, *Nat. Nanotechnol.*, 2021, **16**, 1318–1329.
- 2 K. A. Brown, S. Brittman, N. Maccaferri, D. Jariwala and U. Celano, *Nano Lett.*, 2020, **20**, 2–10.
- 3 C. Toumey, *Nat. Nanotechnol.*, 2020, **15**, 250–251.
- 4 C. R. Kagan, L. E. Fernandez, Y. Gogotsi, P. T. Hammond, M. C. Hersam, A. E. Nel, R. M. Penner, C. G. Willson and P. S. Weiss, *ACS Nano*, 2016, **10**, 9093–9103.
- 5 S. Rigo, C. Cai, G. Gunkel-Grabole, L. Maurizi, X. Zhang, J. Xu and C. G. Palivan, *Adv. Sci.*, 2018, **5**, 1700892.
- 6 A. P. Alivisatos, *ACS Nano*, 2008, **2**, 1514–1516.
- 7 A.-A. E. Mel, P.-Y. Tessier, M. Buffiere, E. Gautron, J. Ding, K. Du, C.-H. Choi, S. Konstantinidis, R. Snyders, C. Bittencourt and L. Molina-Luna, *Small*, 2016, **12**, 2885–2892.
- 8 Y. Peng, T. Cullis and B. Inkson, *Nano Lett.*, 2009, **9**, 91–96.
- 9 P. Happel, T. Waag, M. Schimke, S. Schweißberg, A. Muzha, K. Fortak, D. Heesch, L. Klask, M. Pilscheuer, F. Hoppe, T. Lenders, J. Meijer, G. Lepperdinger and A. Krueger, *Adv. Funct. Mater.*, 2018, **28**, 1802873.
- 10 Y. Jiang, H. Su, W. Wei, Y. Wang, H.-Y. Chen and W. Wang, *Proc. Natl. Acad. Sci. U. S. A.*, 2019, **116**, 6630–6634.

11 D. Guo, G. Xie and J. Luo, *J. Phys. D: Appl. Phys.*, 2013, **47**, 013001.

12 L. Nicole, C. Laberty-Robert, L. Rozes and C. Sanchez, *Nanoscale*, 2014, **6**, 6267–6292.

13 E. Salimi and M. N. Z. Abidin, *Functional Hybrid Nanomaterials for Environmental Remediation*, 2021, pp. 56–78.

14 V. P. Ananikov, *Nanomaterials*, 2019, **9**, 1197.

15 N. Zhao, L. Yan, X. Zhao, X. Chen, A. Li, D. Zheng, X. Zhou, X. Dai and F.-J. Xu, *Chem. Rev.*, 2019, **119**, 1666–1762.

16 H. S. Han, K. Y. Choi, H. Lee, M. Lee, J. Y. An, S. Shin, S. Kwon, D. S. Lee and J. H. Park, *ACS Nano*, 2016, **10**, 10858–10868.

17 S. Yadav, A. K. Sharma and P. Kumar, *Front. Bioeng. Biotechnol.*, 2020, **8**, 127.

18 A. C. Mendes, E. T. Baran, R. L. Reis and H. S. Azevedo, *Wiley Interdiscip. Rev.: Nanomed. Nanobiotechnol.*, 2013, **5**, 582–612.

19 D. Bobo, K. J. Robinson, J. Islam, K. J. Thurecht and S. R. Corrie, *Pharm. Res.*, 2016, **33**, 2373–2387.

20 B. S. Bolu, R. Sanyal and A. Sanyal, *Molecules*, 2018, **23**, 1570.

21 C. Bissantz, B. Kuhn and M. Stahl, *J. Med. Chem.*, 2010, **53**, 5061–5084.

22 B. Du, X. Chen, B. Zhao, A. Mei, Q. Wang, J. Xu and Z. Fan, *Nanoscale*, 2010, **2**, 1684–1689.

23 C. Yi, Y. Yang, B. Liu, J. He and Z. Nie, *Chem. Soc. Rev.*, 2020, **49**, 465–508.

24 Q. Wang, X. Zhao, Y.-I. Lee and H.-G. Liu, *RSC Adv.*, 2015, **5**, 86564–86571.

25 C. Yi, S. Zhang, K. T. Webb and Z. Nie, *Acc. Chem. Res.*, 2017, **50**, 12–21.

26 Y. Liu, Y. Liu, J.-J. Yin and Z. Nie, *Macromol. Rapid Commun.*, 2015, **36**, 711–725.

27 J. He, X. Huang, Y.-C. Li, Y. Liu, T. Babu, M. A. Aronova, S. Wang, Z. Lu, X. Chen and Z. Nie, *J. Am. Chem. Soc.*, 2013, **135**, 7974–7984.

28 T. Bian, L. Shang, H. Yu, M. T. Perez, L.-Z. Wu, C.-H. Tung, Z. Nie, Z. Tang and T. Zhang, *Adv. Mater.*, 2014, **26**, 5613–5618.

29 J. Song, J. Zhou and H. Duan, *J. Am. Chem. Soc.*, 2012, **134**, 13458–13469.

30 J. Song, L. Pu, J. Zhou, B. Duan and H. Duan, *ACS Nano*, 2013, **7**, 9947–9960.

31 W.-M. Wan, C.-Y. Hong and C.-Y. Pan, *Chem. Commun.*, 2009, 5883–5885.

32 M. Chen, J.-W. Li, W.-J. Zhang, C.-Y. Hong and C.-Y. Pan, *Macromolecules*, 2019, **52**, 1140–1149.

33 W.-D. He, X.-L. Sun, W.-M. Wan and C.-Y. Pan, *Macromolecules*, 2011, **44**, 3358–3365.

34 J. Kadirkhanov, C.-L. Yang, Z.-X. Chang, R.-M. Zhu, C.-Y. Pan, Y.-Z. You, W.-J. Zhang and C.-Y. Hong, *Polym. Chem.*, 2021, **12**, 1768–1775.

35 Y. Li and S. P. Armes, *Angew. Chem., Int. Ed.*, 2010, **49**, 4042–4046.

36 A. Blanazs, R. Verber, O. O. Mykhaylyk, A. J. Ryan, J. Z. Heath, C. W. I. Douglas and S. P. Armes, *J. Am. Chem. Soc.*, 2012, **134**, 9741–9748.

37 C. Gonzato, M. Semsarilar, E. R. Jones, F. Li, G. J. P. Krooshof, P. Wyman, O. O. Mykhaylyk, R. Tuinier and S. P. Armes, *J. Am. Chem. Soc.*, 2014, **136**, 11100–11106.

38 L. A. Fielding, J. A. Lane, M. J. Derry, O. O. Mykhaylyk and S. P. Armes, *J. Am. Chem. Soc.*, 2014, **136**, 5790–5798.

39 A. Czajka and S. P. Armes, *J. Am. Chem. Soc.*, 2021, **143**, 1474–1484.

40 C. J. Mable, L. A. Fielding, M. J. Derry, O. O. Mykhaylyk, P. Chambon and S. P. Armes, *Chem. Sci.*, 2018, **9**, 1454–1463.

41 W. Zhou, Q. Qu, Y. Xu and Z. An, *ACS Macro Lett.*, 2015, **4**, 495–499.

42 Y. Li, Z. Ye, L. Shen, Y. Xu, A. Zhu, P. Wu and Z. An, *Macromolecules*, 2016, **49**, 3038–3048.

43 X. Wang, C. A. Figg, X. Lv, Y. Yang, B. S. Sumerlin and Z. An, *ACS Macro Lett.*, 2017, **6**, 337–342.

44 F. Lv, Z. An and P. Wu, *Nat. Commun.*, 2019, **10**, 1397.

45 B. Zhang, X. Lv and Z. An, *ACS Macro Lett.*, 2017, **6**, 224–228.

46 M. Cao, H. Nie, Y. Hou, G. Han and W. Zhang, *Polym. Chem.*, 2019, **10**, 403–411.

47 C. Gao, J. Wu, H. Zhou, Y. Qu, B. Li and W. Zhang, *Macromolecules*, 2016, **49**, 4490–4500.

48 S. Li, X. He, Q. Li, P. Shi and W. Zhang, *ACS Macro Lett.*, 2014, **3**, 916–921.

49 S. Qu, K. Wang, H. Khan, W. Xiong and W. Zhang, *Polym. Chem.*, 2019, **10**, 1150–1157.

50 P. Shi, Y. Qu, C. Liu, H. Khan, P. Sun and W. Zhang, *ACS Macro Lett.*, 2016, **5**, 88–93.

51 Y. Ding, M. Cai, Z. Cui, L. Huang, L. Wang, X. Lu and Y. Cai, *Angew. Chem., Int. Ed.*, 2018, **57**, 1053–1056.

52 M. Cai, Y. Ding, L. Wang, L. Huang, X. Lu and Y. Cai, *ACS Macro Lett.*, 2018, **7**, 208–212.

53 L. Huang, Y. Ding, Y. Ma, L. Wang, Q. Liu, X. Lu and Y. Cai, *Macromolecules*, 2019, **52**, 4703–4712.

54 L. Wang, Y. Ding, Q. Liu, Q. Zhao, X. Dai, X. Lu and Y. Cai, *ACS Macro Lett.*, 2019, **8**, 623–628.

55 X. Chen, L. Liu, M. Huo, M. Zeng, L. Peng, A. Feng, X. Wang and J. Yuan, *Angew. Chem., Int. Ed.*, 2017, **56**, 16541–16545.

56 M. Huo, Q. Ye, H. Che, X. Wang, Y. Wei and J. Yuan, *Macromolecules*, 2017, **50**, 1126–1133.

57 M. Huo, M. Zeng, D. Li, L. Liu, Y. Wei and J. Yuan, *Macromolecules*, 2017, **50**, 8212–8220.

58 S. Guan and A. Chen, *Macromolecules*, 2020, **53**, 6235–6245.

59 L. D. Blackman, K. E. B. Doncom, M. I. Gibson and R. K. O'Reilly, *Polym. Chem.*, 2017, **8**, 2860–2871.

60 S. Varlas, J. C. Foster, P. G. Georgiou, R. Keogh, J. T. Husband, D. S. Williams and R. K. O'Reilly, *Nanoscale*, 2019, **11**, 12643–12654.

61 L. D. Blackman, S. Varlas, M. C. Arno, Z. H. Houston, N. L. Fletcher, K. J. Thurecht, M. Hasan, M. I. Gibson and R. K. O'Reilly, *ACS Cent. Sci.*, 2018, **4**, 718–723.

62 S. Varlas, R. Keogh, Y. Xie, S. L. Horswell, J. C. Foster and R. K. O'Reilly, *J. Am. Chem. Soc.*, 2019, **141**, 20234–20248.

63 J. Yeow, J. Xu and C. Boyer, *ACS Macro Lett.*, 2015, **4**, 984–990.

64 J. Yeow, O. R. Sugita and C. Boyer, *ACS Macro Lett.*, 2016, **5**, 558–564.

65 S. Xu, G. Ng, J. Xu, R. P. Kuchel, J. Yeow and C. Boyer, *ACS Macro Lett.*, 2017, **6**, 1237–1244.

66 N. Zaquet, J. Yeow, T. Junkers, C. Boyer and P. B. Zetterlund, *Macromolecules*, 2018, **51**, 5165–5172.

67 S. Dong, W. Zhao, F. P. Lucien, S. Perrier and P. B. Zetterlund, *Polym. Chem.*, 2015, **6**, 2249–2254.

68 D. Zhou, R. P. Kuchel and P. B. Zetterlund, *Polym. Chem.*, 2017, **8**, 4177–4181.

69 G. K. K. Clothier, T. R. Guimarães, M. Khan, G. Moad, S. Perrier and P. B. Zetterlund, *ACS Macro Lett.*, 2019, **8**, 989–995.

70 T. R. Guimarães, M. Khan, R. P. Kuchel, I. C. Morrow, H. Minami, G. Moad, S. Perrier and P. B. Zetterlund, *Macromolecules*, 2019, **52**, 2965–2974.

71 M. A. Touve, C. A. Figg, D. B. Wright, C. Park, J. Cantlon, B. S. Sumerlin and N. C. Gianneschi, *ACS Cent. Sci.*, 2018, **4**, 543–547.

72 J. Y. Rho, G. M. Scheutz, S. Häkkinen, J. B. Garrison, Q. Song, J. Yang, R. Richardson, S. Perrier and B. S. Sumerlin, *Polym. Chem.*, 2021, **12**, 3947–3952.

73 C. A. Figg, A. Simula, K. A. Gebre, B. S. Tucker, D. M. Haddleton and B. S. Sumerlin, *Chem. Sci.*, 2015, **6**, 1230–1236.

74 J. Cao, Y. Tan, X. Dai, Y. Chen, L. Zhang and J. Tan, *Polymer*, 2021, **230**, 124095.

75 X. Luo, S. Zhao, Y. Chen, L. Zhang and J. Tan, *Macromolecules*, 2021, **54**, 2948–2959.

76 S. Han, J. Wu, Y. Zhang, J. Lai, Y. Chen, L. Zhang and J. Tan, *Macromolecules*, 2021, **54**, 4669–4681.

77 J. Cao, Y. Tan, Y. Chen, L. Zhang and J. Tan, *Macromol. Rapid Commun.*, 2021, **42**, 2100333.

78 J. He, D. Lin, Y. Chen, L. Zhang and J. Tan, *Macromol. Rapid Commun.*, 2021, **42**, 2100201.

79 R. Zeng, Y. Chen, L. Zhang and J. Tan, *Macromolecules*, 2020, **53**, 1557–1566.

80 Q. Zhang, R. Zeng, Y. Zhang, Y. Chen, L. Zhang and J. Tan, *Macromolecules*, 2020, **53**, 8982–8991.

81 D. Liu, Y. Chen, L. Zhang and J. Tan, *Macromolecules*, 2020, **53**, 9725–9735.

82 D. Liu, W. Cai, L. Zhang, C. Boyer and J. Tan, *Macromolecules*, 2020, **53**, 1212–1223.

83 C. J. Ferguson, R. J. Hughes, B. T. T. Pham, B. S. Hawkett, R. G. Gilbert, A. K. Serelis and C. H. Such, *Macromolecules*, 2002, **35**, 9243–9245.

84 G. Wang, M. Schmitt, Z. Wang, B. Lee, X. Pan, L. Fu, J. Yan, S. Li, G. Xie, M. R. Bockstaller and K. Matyjaszewski, *Macromolecules*, 2016, **49**, 8605–8615.

85 Y. Wang, G. Han, W. Duan and W. Zhang, *Macromol. Rapid Commun.*, 2019, **40**, 1800140.

86 C. Dire, S. Magnet, L. Couvreur and B. Charleux, *Macromolecules*, 2009, **42**, 95–103.

87 G. Delaittre, C. Dire, J. Rieger, J.-L. Putaux and B. Charleux, *Chem. Commun.*, 2009, 2887–2889.

88 D. B. Wright, M. A. Touve, L. Adamiak and N. C. Gianneschi, *ACS Macro Lett.*, 2017, **6**, 925–929.

89 S. Varlas, J. C. Foster, L. A. Arkinstall, J. R. Jones, R. Keogh, R. T. Mathers and R. K. O'Reilly, *ACS Macro Lett.*, 2019, **8**, 466–472.

90 J. Jiang, X. Zhang, Z. Fan and J. Du, *ACS Macro Lett.*, 2019, **8**, 1216–1221.

91 C. Grazon, P. Salas-Ambrosio, E. Ibarboure, A. Buol, E. Garanger, M. W. Grinstaff, S. Lecommandoux and C. Bonduelle, *Angew. Chem., Int. Ed.*, 2020, **59**, 622–626.

92 J. Wang, M. Cao, P. Zhou and G. Wang, *Macromolecules*, 2020, **53**, 3157–3165.

93 Y. Kitayama, A. Chaiyasat, H. Minami and M. Okubo, *Macromolecules*, 2010, **43**, 7465–7471.

94 W.-J. Zhang, C.-Y. Hong and C.-Y. Pan, *Macromol. Rapid Commun.*, 2019, **40**, 1800279.

95 J.-T. Sun, C.-Y. Hong and C.-Y. Pan, *Polym. Chem.*, 2013, **4**, 873–881.

96 B. Charleux, G. Delaittre, J. Rieger and F. D'Agosto, *Macromolecules*, 2012, **45**, 6753–6765.

97 N. J. Warren and S. P. Armes, *J. Am. Chem. Soc.*, 2014, **136**, 10174–10185.

98 S. L. Canning, G. N. Smith and S. P. Armes, *Macromolecules*, 2016, **49**, 1985–2001.

99 N. J. W. Penfold, J. Yeow, C. Boyer and S. P. Armes, *ACS Macro Lett.*, 2019, **8**, 1029–1054.

100 M. J. Derry, L. A. Fielding and S. P. Armes, *Prog. Polym. Sci.*, 2016, **52**, 1–18.

101 X. Wang, L. Shen and Z. An, *Prog. Polym. Sci.*, 2018, **83**, 1–27.

102 D. Liu, J. He, L. Zhang and J. Tan, *ACS Macro Lett.*, 2019, **8**, 1660–1669.

103 J. Cao, Y. Tan, Y. Chen, L. Zhang and J. Tan, *Macromol. Rapid Commun.*, 2021, **42**, 2100498.

104 F. D'Agosto, J. Rieger and M. Lansalot, *Angew. Chem., Int. Ed.*, 2020, **59**, 8368–8392.

105 G. Cheng and J. Pérez-Mercader, *Macromol. Rapid Commun.*, 2019, **40**, 1800513.

106 S. Y. Khor, J. F. Quinn, M. R. Whittaker, N. P. Truong and T. P. Davis, *Macromol. Rapid Commun.*, 2019, **40**, 1800438.

107 D. Le, D. Keller and G. Delaittre, *Macromol. Rapid Commun.*, 2019, **40**, 1800551.

108 J. Huang, Y. Guo, S. Gu, G. Han, W. Duan, C. Gao and W. Zhang, *Polym. Chem.*, 2019, **10**, 3426–3435.

109 P. B. Zetterlund, S. C. Thickett, S. Perrier, E. Bourgeat-Lami and M. Lansalot, *Chem. Rev.*, 2015, **115**, 9745–9800.

110 F. Jasinski, P. B. Zetterlund, A. M. Braun and A. Chemtob, *Prog. Polym. Sci.*, 2018, **84**, 47–88.

111 J. Yeow and C. Boyer, *Adv. Sci.*, 2017, **4**, 1700137.

112 N. An, X. Chen and J. Yuan, *Polym. Chem.*, 2021, **12**, 3220–3232.

113 S. C. Thickett and G. H. Teo, *Polym. Chem.*, 2019, **10**, 2906–2924.

114 C. Liu, C.-Y. Hong and C.-Y. Pan, *Polym. Chem.*, 2020, **11**, 3673–3689.

115 Y. Ning and S. P. Armes, *Acc. Chem. Res.*, 2020, **53**, 1176–1186.

116 W. Zhou, Q. Qu, W. Yu and Z. An, *ACS Macro Lett.*, 2014, **3**, 1220–1224.

117 J. Huang, D. Liu, Y. Chen, L. Zhang and J. Tan, *Macromol. Rapid Commun.*, 2021, **42**, 2000720.

118 M. Semsarilar, E. R. Jones, A. Blanazs and S. P. Armes, *Adv. Mater.*, 2012, **24**, 3378–3382.

119 B. Karagoz, J. Yeow, L. Esser, S. M. Prakash, R. P. Kuchel, T. P. Davis and C. Boyer, *Langmuir*, 2014, **30**, 10493–10502.

120 L. Yu, Y. Zhang, X. Dai, L. Zhang and J. Tan, *Chem. Commun.*, 2019, **55**, 7848–7851.

121 M. Tan, Y. Shi, Z. Fu and W. Yang, *Polym. Chem.*, 2018, **9**, 1082–1094.

122 R. Bleach, B. Karagoz, S. M. Prakash, T. P. Davis and C. Boyer, *ACS Macro Lett.*, 2014, **3**, 591–596.

123 W.-J. Zhang, C.-Y. Hong and C.-Y. Pan, *J. Mater. Chem. A*, 2014, **2**, 7819–7828.

124 Y. Zhang, Z. Wang, K. Matyjaszewski and J. Pietrasik, *Eur. Polym. J.*, 2019, **110**, 49–55.

125 A. Rubio, G. Desnos and M. Semsarilar, *Macromol. Chem. Phys.*, 2018, **219**, 1800351.

126 L. Yu, Y. Zhang, X. Dai, Q. Xu, L. Zhang and J. Tan, *Chem. Commun.*, 2019, **55**, 11920–11923.

127 J. Huang, D. Li, H. Liang and J. Lu, *Macromol. Rapid Commun.*, 2017, **38**, 1700202.

128 J. Wan, B. Fan and S. H. Thang, *Nanoscale Adv.*, 2021, **3**, 3306–3315.

129 B. Fan, Y. Liu, J. Wan, S. Crawford and S. H. Thang, *ACS Mater. Lett.*, 2020, **2**, 492–498.

130 P. Shi, C. Gao, X. He, P. Sun and W. Zhang, *Macromolecules*, 2015, **48**, 1380–1389.

131 C. Huang, J. Tan, Q. Xu, J. He, X. Li, D. Liu and L. Zhang, *RSC Adv.*, 2017, **7**, 46069–46081.

132 J. Tan, D. Liu, C. Huang, X. Li, J. He, Q. Xu and L. Zhang, *Macromol. Rapid Commun.*, 2017, **38**, 1700195.

133 B. Shi, H. Zhang, Y. Liu, J. Wang, P. Zhou, M. Cao and G. Wang, *Macromol. Rapid Commun.*, 2019, **40**, 1900547.

134 G. H. Teo, R. P. Kuchel, P. B. Zetterlund and S. C. Thickett, *Polym. Chem.*, 2016, **7**, 6575–6585.

135 J. Tan, X. Li, R. Zeng, D. Liu, Q. Xu, J. He, Y. Zhang, X. Dai, L. Yu, Z. Zeng and L. Zhang, *ACS Macro Lett.*, 2018, **7**, 255–262.

136 X. Luo, K. Zhang, R. Zeng, Y. Chen, L. Zhang and J. Tan, *Macromolecules*, 2022, **55**, 65–77.

137 S. Berger, O. Ornatsky, V. Baranov, M. A. Winnik and A. Pich, *J. Mater. Chem.*, 2010, **20**, 5141–5150.

138 H. Kong and J. Jang, *Biomacromolecules*, 2008, **9**, 2677–2681.

139 Q. Xu, Y. Zhang, X. Li, J. He, J. Tan and L. Zhang, *Polym. Chem.*, 2018, **9**, 4908–4916.

140 C. Song, Y. Sun, J. Li, C. Dong, J. Zhang, X. Jiang and L. Wang, *Nanoscale*, 2019, **11**, 18881–18893.

141 X. Wang, C. Wang, L. Cheng, S.-T. Lee and Z. Liu, *J. Am. Chem. Soc.*, 2012, **134**, 7414–7422.

142 B. B. Sahoo, N. Kumar, H. S. Panda, B. Panigrahy, N. K. Sahoo, A. Soam, B. S. Mahanto and P. K. Sahoo, *J. Energy Storage*, 2021, **43**, 103157.

143 C. Gao, Q. Zhang, Z. Lu and Y. Yin, *J. Am. Chem. Soc.*, 2011, **133**, 19706–19709.

144 Z. Shu, Y. Chen, J. Zhou, T. Li, Z. Sheng, C. Tao and Y. Wang, *Appl. Clay Sci.*, 2016, **132–133**, 114–121.

145 N. Zhang, Y. Qiu, H. Sun, J. Hao, J. Chen, J. Xi, J. Liu, B. He and Z.-W. Bai, *ACS Appl. Nano Mater.*, 2021, **4**, 5854–5863.

146 X. Chen, R. Klingeler, M. Kath, A. A. El Gendy, K. Cendrowski, R. J. Kalenczuk and E. Borowiak-Palen, *ACS Appl. Mater. Interfaces*, 2012, **4**, 2303–2309.

147 B. Ebeling and P. Vana, *Macromolecules*, 2013, **46**, 4862–4871.

148 W. Peng, C. Rossner, V. Roddatis and P. Vana, *ACS Macro Lett.*, 2016, **5**, 1227–1231.

149 Y. Zhu, B. Yang, S. Chen and J. Du, *Prog. Polym. Sci.*, 2017, **64**, 1–22.

150 J. He, J. Cao, Y. Chen, L. Zhang and J. Tan, *ACS Macro Lett.*, 2020, **9**, 533–539.

151 H. Che and J. C. M. van Hest, *J. Mater. Chem. B*, 2016, **4**, 4632–4647.

152 J. Tan, D. Liu, Y. Bai, C. Huang, X. Li, J. He, Q. Xu, X. Zhang and L. Zhang, *Polym. Chem.*, 2017, **8**, 1315–1327.

153 A. Blanazs, A. J. Ryan and S. P. Armes, *Macromolecules*, 2012, **45**, 5099–5107.

154 J. Tan, D. Liu, Y. Bai, C. Huang, X. Li, J. He, Q. Xu and L. Zhang, *Macromolecules*, 2017, **50**, 5798–5806.

155 A. Blanazs, J. Madsen, G. Battaglia, A. J. Ryan and S. P. Armes, *J. Am. Chem. Soc.*, 2011, **133**, 16581–16587.

156 J. Tan, H. Sun, M. Yu, B. S. Sumerlin and L. Zhang, *ACS Macro Lett.*, 2015, **4**, 1249–1253.

157 J. Tan, D. Liu, X. Zhang, C. Huang, J. He, Q. Xu, X. Li and L. Zhang, *RSC Adv.*, 2017, **7**, 23114–23121.

158 J. Tan, Q. Xu, X. Li, J. He, Y. Zhang, X. Dai, L. Yu, R. Zeng and L. Zhang, *Macromol. Rapid Commun.*, 2018, **39**, 1700871.

159 C. J. Mable, R. R. Gibson, S. Prevost, B. E. McKenzie, O. O. Mykhaylyk and S. P. Armes, *J. Am. Chem. Soc.*, 2015, **137**, 16098–16108.

160 Z. Ding, M. Ding, C. Gao, C. Boyer and W. Zhang, *Macromolecules*, 2017, **50**, 7593–7602.

161 S. Rose, A. Prevoteau, P. Elzière, D. Hourdet, A. Marcellan and L. Leibler, *Nature*, 2014, **505**, 382–385.

162 C. J. Mable, M. J. Derry, K. L. Thompson, L. A. Fielding, O. O. Mykhaylyk and S. P. Armes, *Macromolecules*, 2017, **50**, 4465–4473.

163 R. Deng, M. J. Derry, C. J. Mable, Y. Ning and S. P. Armes, *J. Am. Chem. Soc.*, 2017, **139**, 7616–7623.

164 E. E. Brotherton, F. L. Hatton, A. A. Cockram, M. J. Derry, A. Czajka, E. J. Cornel, P. D. Topham, O. O. Mykhaylyk and S. P. Armes, *J. Am. Chem. Soc.*, 2019, **141**, 13664–13675.

165 X. Dai, L. Yu, Y. Zhang, L. Zhang and J. Tan, *Macromolecules*, 2019, **52**, 7468–7476.

166 J. Tan, X. Dai, Y. Zhang, L. Yu, H. Sun and L. Zhang, *ACS Macro Lett.*, 2019, **8**, 205–212.

167 D. Nguyen, V. Huynh, M. Lam, A. Serelis, T. Davey, O. Paravagna, C. Such and B. Hawkett, *Macromol. Rapid Commun.*, 2021, **42**, 2170036.

168 Y. Ning, L. Han, M. J. Derry, F. C. Meldrum and S. P. Armes, *J. Am. Chem. Soc.*, 2019, **141**, 2557–2567.

169 J. Tan, C. Huang, D. Liu, X. Li, J. He, Q. Xu and L. Zhang, *ACS Macro Lett.*, 2017, **6**, 298–303.

170 B. Yuan, X. He, Y. Qu, C. Gao, E. Eiser and W. Zhang, *Polym. Chem.*, 2017, **8**, 2173–2181.

171 A. Zhu, X. Lv, L. Shen, B. Zhang and Z. An, *ACS Macro Lett.*, 2017, **6**, 304–309.

172 J. Tan, Q. Xu, Y. Zhang, C. Huang, X. Li, J. He and L. Zhang, *Macromolecules*, 2018, **51**, 7396–7406.

173 Y. Zheng, Y. Huang, Z. M. Abbas and B. C. Benicewicz, *Polym. Chem.*, 2016, **7**, 5347–5350.

174 Y. Zheng, Y. Huang, Z. M. Abbas and B. C. Benicewicz, *Polym. Chem.*, 2017, **8**, 370–374.

175 J. Wang, B. Zhu, Y. Wang, Y. Hao, J. Zhang and Z. Li, *Soft Matter*, 2021, **18**, 97–106.

176 W. Hou, H. Wang, Y. Cui, Y. Liu, X. Ma and H. Zhao, *Macromolecules*, 2019, **52**, 8404–8414.

177 W. Hou, W. Zhong and H. Zhao, *Macromolecules*, 2021, **54**, 2617–2626.

178 X. G. Qiao, P.-Y. Dugas, B. Charleux, M. Lansalot and E. Bourgeat-Lami, *Macromolecules*, 2015, **48**, 545–556.

179 X. G. Qiao, O. Lambert, J.-C. Taveau, P.-Y. Dugas, B. Charleux, M. Lansalot and E. Bourgeat-Lami, *Macromolecules*, 2017, **50**, 3796–3806.

180 E. Bourgeat-Lami, A. J. P. G. França, T. C. Chaparro, R. D. Silva, P.-Y. Dugas, G. M. Alves and A. M. Santos, *Macromolecules*, 2016, **49**, 4431–4440.

181 L. Upadhyaya, C. Egbosimba, X. Qian, R. Wickramasinghe, R. Fernández-Pacheco, I. M. Coelhoso, C. A. M. Portugal, J. G. Crespo, D. Quemener and M. Semsarilar, *Macromol. Rapid Commun.*, 2019, **40**, 1800333.

182 Z. Liu, C. Wu, Y. Fu, X. Xu, J. Ying, J. Sheng, Y. Huang, C. Ma and T. Chen, *Nanoscale Adv.*, 2021, **3**, 347–352.

183 A. M. Oliver, J. Gwyther, C. E. Boott, S. Davis, S. Pearce and I. Manners, *J. Am. Chem. Soc.*, 2018, **140**, 18104–18114.